Dissimilar Materials Joining of Al Alloy/ CFRTP by Friction Lap Joining†

NAGATSUKA Kimiaki*, BOLYU Xiao, TSUCHIYA Atsuki***, TSUKAMOTO Masahiro**** and NAKATA Kazuhiro*****

Abstract

Carbon fiber reinforced thermoplastics, which consisted of the polyamide 6 as the matrix and 20wt% carbon fiber, and A5052 plates were directly joined by the friction lap joining method. A continuous joined interface of A5052/CFRTP joint was obtained at various tool rotation speeds ranging from 1000 to 2500 rpm. These materials were joined by bonding of MgO oxide layer of A5052 and PA6 as the matrix of the CFRTP. Voids were observed in the CFRTP at the interface of the joint, and its quantity increased with increasing tool rotation speed. The tensile shear fracture load of the FLJ joint increased with increasing the tool rotation speed from 1000 to 2000 rpm, and then it decreased. The fracture mainly occurred at the joint interface, however, some joints joined at the tool rotation speed of 2000 and 2500 rpm showed the CFRTP base plate fracture.

KEY WORDS: (Friction lap joining), (CFRTP), (Al alloy), (Dissimilar materials joining)

1. Introduction

Carbon fiber reinforced plastics (CFRPs) have several superior characteristics such as light weight and remarkable mechanical properties compared to conventional metal materials, hence, they have been introduced as novel structural materials in automobiles and aircraft [1-3]. In particular, carbon fiber reinforced thermoplastics (CFRTPs), which are composite materials of carbon fibers and thermoplastic matrix such as polyamide (PA6), polyethylene (PE), polyphenylene sulfide (PPS), can be formed using an injection molding method with large specific tensile strengths and several polymer materials properties [3]. Dissimilar materials joining techniques for bonding metals to CFRTPs have been demanded to expand the range of applications for CFRTPs and improve their manufacturing production and performance characteristics.

Adhesive bonding and mechanical fastening have been used for joining metals to plastic materials including CFRTPs [4-10]. However, these joining techniques have several problems such as the environmental pollutants and requiring long processing times in adhesive bonding, and stress concentrations, low air-tightness, increase of weight and not suitable for many mass production schemes in mechanical fastening.

The direct joining of metals to plastic materials have been investigated recently such as a laser joining [8-14], ultrasonic welding [15-17], induction heating [18], friction spot joining [19, 20] and friction lap joining (FLJ)[21-25] to solve these problems.

In these process, FLJ has several advantages such as a low cost and simple equipment, and a low joint geometry restriction [21-25]. FLJ uses the heat energy generated by friction between the rotating tool and metal surface. A rotating tool is pressed on the metal surface and travels along the joining line. During tool traveling the plastic is heated and melted by the heat transfer from the heated metal. The tool generates not only the heat input but also the pressure to the joint interface. Joining

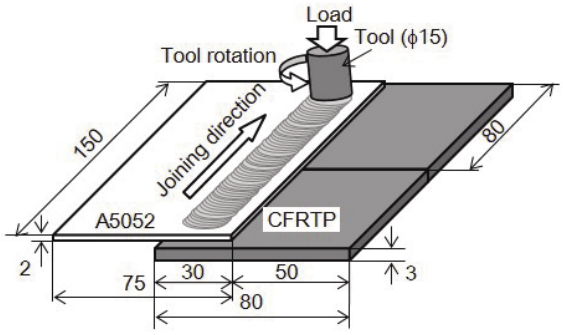

Fig. 1 Schematic illustration of FLJ apparatus.

† Received on July 31, 2015
* Specially Appointed Assistant Professor
** Researcher, **** Toray Industries, Inc.
**** Associate Professor
***** Specially Appointed Professor
Transactions of JWRI is published by Joining and Welding Research Institute, Osaka University, Ibaraki, Osaka 567-0047, Japan

of the metal and the plastic is completed after the melted plastic is solidified under the pressure.

The purpose of this study was to confirm the possibility of directly joining CFRTPs and Al alloys using the FLJ technique, and the effect of the tool rotation speed as the major process parameter on the joint characteristics was investigated. Al alloy was used as the metal substrate of the CFRTP/metal component due to its light weight, high strength and good formability, which are important when considering the fabrication of automobiles and aircraft [26].

2. Experimental

Experimental materials were A5052 Al alloy plates (150 mm × 75 mm × 2 mm) with a composition of 2.4 mass% Mg and 0.18 mass% Cr, and injection-molded CFRTP plates (80 mm × 80 mm × 3 mm) of polyamide 6 with a 20 mass% carbon fiber addition. The diameter and length of these carbon fibers were 10 μm and approximately 500 μm, respectively. As the surface treatment, the surface of A5052 plate was wet ground by #800 emery paper in water. Wet-ground A5052 and CFRTP plates were degreased using ethanol before the joining process. **Fig. 1** shows the schematic illustration of FLJ apparatus. A5052 plate was placed on the CFRTP plates as shown in Fig. 1. FLJ was used to join the A5052 plate to the CFRTP plate using a rotating tool made of SKD tool steel with shoulder diameter of 15 mm and without probe. This tool was tilted at an angle 3° forward from the vertical. A tool plunge depth of 0.9 mm was employed to ensure the contact between the tool and the plate surface of A5052. A joining speed was fixed at 1600 mm/min and different tool rotation speeds in the range 1000-2500 rpm were employed. The temperature during FLJ was monitored using a K-type thermocouple inserted at the ground-A5052 plate/CFRTP plate interface at the center of the joined area. Observations of the appearance and the cross-sectional microstructure of the FLJ-joined specimens were performed using optical microscope (OM), scanning electron microscope and transmission electron microscope (TEM). To evaluate the joint strength in the tensile shear test, the FLJ joints were cut into strips perpendicular to the joining direction with a width of 15 mm. Three strips were tested for each joining condition. The fractured surfaces were analyzed using OM and SEM.

3. Results and Discussion

3.1 Temperature history during FLJ

Fig. 2 shows the temperature histories during FLJ at tool rotation speed of 2000 and 2500 rpm. The temperature of the joint interface rapidly increased as the rotating tool approached the midway measurement point. Maximum temperatures of 725 K and 754 K were obtained at tool rotation speed of 2000 and 2500 rpm, respectively. These were above the melting temperature (approximately 498 K) and thermal decomposition temperature (approximately 623 K) of PA6 as the matrix of CFRTP.

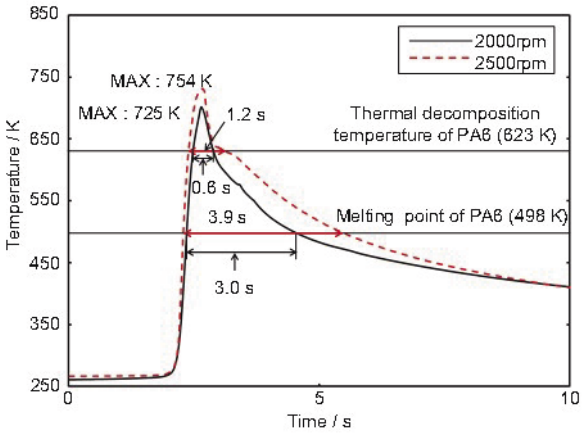

Fig. 2 Temperature histories during FLJ at tool rotation speed of 2000 and 2500 rpm.

Fig. 3 Appearance of the FLJ joint of A5052/CFRTP joined at various tool rotation speeds..

The span of time over which the temperature exceeded the melting and thermal decomposition temperature of PA6 increased with increasing the tool rotation speed. The increase in tool rotation speed from 2000 rpm to 2500 rpm increased the melting interval from 3.0 to 3.9 s and the thermal-decomposition interval from 0.6 to 1.2 s.

3.2 Appearance and cross-sectional microstructure of CFRTP/A5052 joint

Fig. 3 shows the appearance of the FLJ joint of A5052/CFRTP joined at various tool rotation speeds. The A5052/CFRTP joints were obtained at all the joining conditions. The smooth frictionized area was observed on A5052 surface at tool rotation speed from 1500 to 2500 rpm. A rough surface was observed on the joint at a tool rotation speed of 1000 rpm. The large flash was not confirmed in all the conditions, however, small flash was observed on the joint at 2500 rpm.

Fig. 4 shows the cross-sectional macrostructure of the FLJ joint of A5052/CFRTP joined at various tool rotation speeds. A continuous joined interface of A5052/CFRTP joint was obtained. The concave-downward deformation of the A5052 plate and CFRTP was observed in the tool-passed zone. With increasing tool rotation speed, the

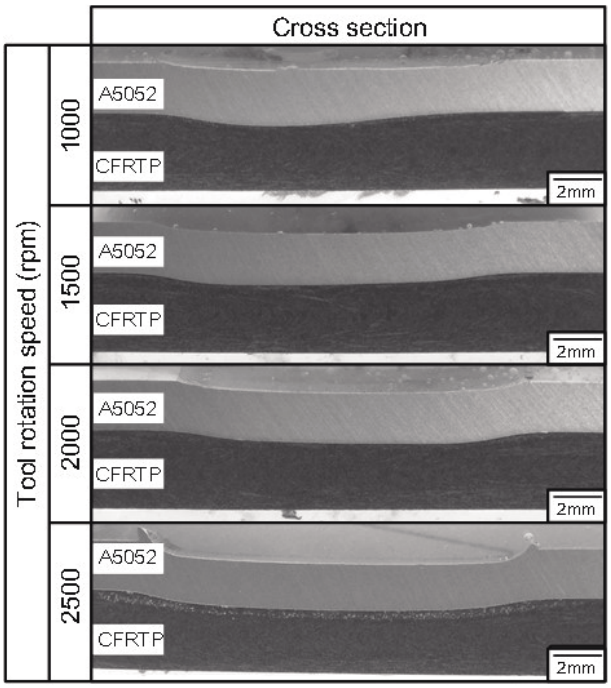

Fig. 4 Cross-sectional macrostructure of the FLJ joint of A5052/CFRTP joined at various tool rotation speeds.

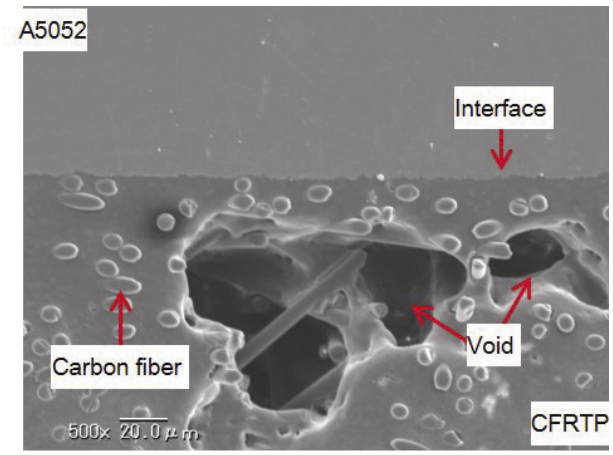

Fig. 5 Secondary electron image (SEI) at the interface of A5052/CFRTP joints joined at the tool rotation speed of 2000 rpm.

concave-downward deformation of the A5052 plate and CFRTP plate increased. In addition, voids were observed beneath the interface in the melted zone of CFRTP, and its quantity increased with increasing tool rotation speed.

Fig. 5 shows the secondary electron image (SEI) at the interface of A5052/CFRTP joints joined at the tool rotation speed of 2000 rpm. The A5052 plate was joined to the CFRTP via PA6. Voids were observed in the melted area of CFRTP near the interface. The inner of these voids showed the smooth surface. These voids would be generated by the volatile products such as H2O and CO2 due to the thermal decomposition of PA6 at

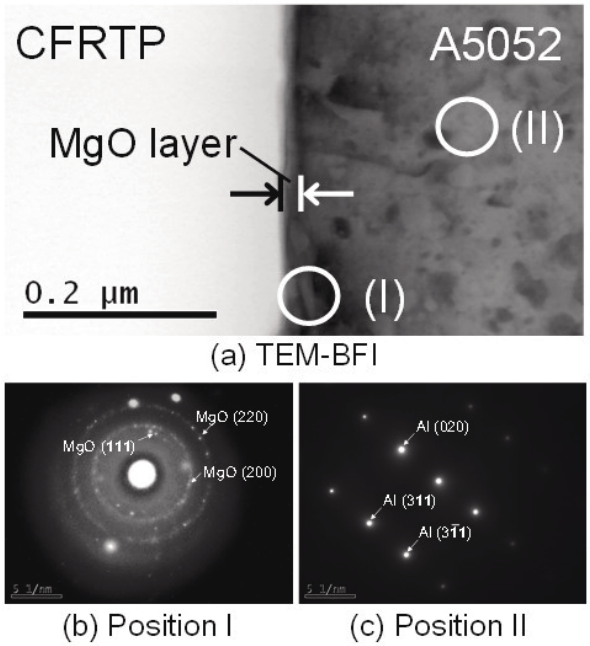

Fig. 6 (a) TEM bright field image (BFI) at the interface of FLJ joint joined at tool rotation speed of 2000rpm, and (b) and (c) selected area diffraction patterns at the position I and II in (a).

temperatures over 573 K [27].

Fig. 6 shows the (a) TEM bright field image (BFI) at the interface of FLJ joint joined at tool rotation speed of 2000rpm, and (b) and (c) selected area diffraction patterns at the position I and II in (a), respectively. The bright left part was PA6 in CFRTP and the dark right part was A5052 in BFI. No voids or gaps were observed at the adhered interface. The CFRTP and A5052 alloy were joined via an oxide layer that consisted of Mg and O. A selected-area diffraction analysis identified the oxide layer as MgO. The formation of MgO could be explained thermodynamically as a result of the following reaction [28] between the superficial oxide layer (Al2O3) and Mg: $Mg+1/3Al_2O_3 \rightarrow MgO+2/3Al$. Not only the anchor (mechanical bonding) effect and Van der Waals interaction force, but also chemical bonding were considered as bonding mechanisms of these materials. Especially, the hydrogen bonding between MgO oxide layer of A5052 and amide group (CONH) in PA6 as the matrix of CFRTP would be the effective joining force [29-31].

3.3 Mechanical properties and fracture morphology of CFRTP/A5052 joints

Fig. 7 shows the relation between the tool rotation speed and the tensile shear fracture load of the FLJ joint. The tensile shear fracture load increased with increasing the tool rotation speed from 1000 to 2000 rpm, and it reached maximum value of 2.9 kN. In higher tool rotation speed, it decreased. Almost all of FLJ joints were fractured at the A5052/CFRTP interface. However, the

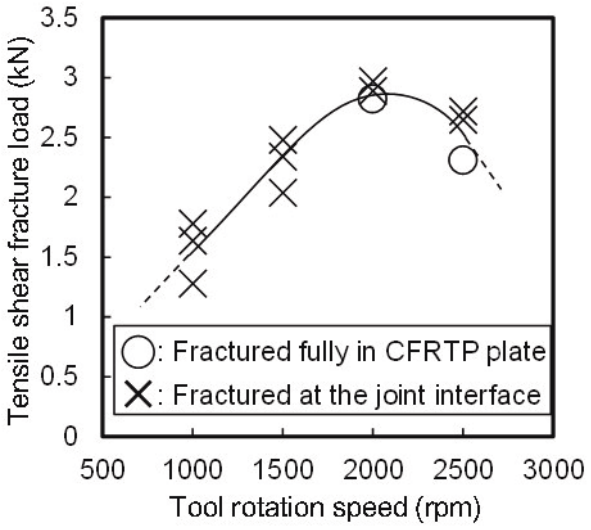

Fig. 7 Relation between the tool rotation speed and the tensile shear fracture load of the FLJ joint.

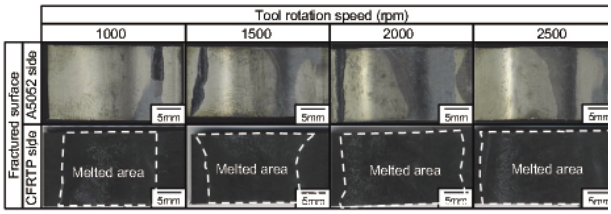

Fig. 8 Fractured surfaces on A5052 and CFRTP sides of fractured FLJ joints after tensile shear test.

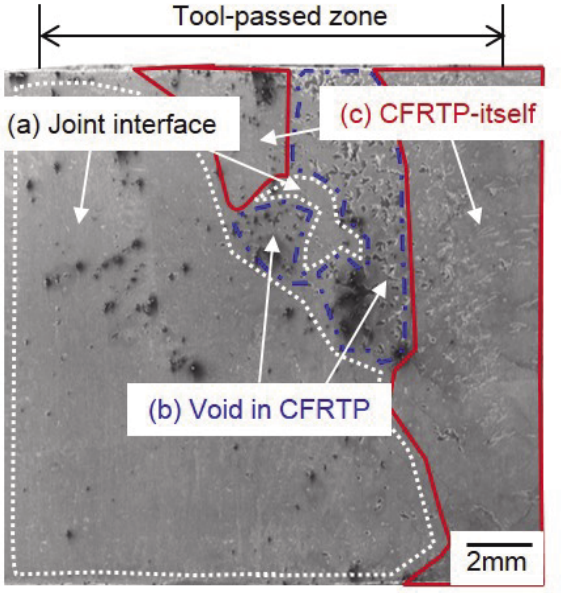

Fig. 9 SEI of the fractured surface in the tool-passed zone on the A5052 side of fractured joint at the tool rotation speed of 2000 rpm.

CFRTP plate fracture also occurred at the tool rotation speeds of 2000 and 2500 rpm. The maximum tensile strength of the joints, which was fractured at the CFRTP base plate, were 60 and 61 MPa for tool rotation speeds of 2000 and 2500 rpm, respectively. These strengths were lower than those of the as-injected CFRTP (140 MPa). This would be caused by the voids formation in CFRTP and the thermal decomposition of PA6 in CFRTP of the joint. **Fig. 8** shows the fractured surfaces on A5052 and CFRTP sides of fractured FLJ joints after tensile shear test. A thin residual CFRTP, which bonded to the surface of A5052, was observed on the fractured surface of the A5052 at all the tool rotation speeds. The melted area of the CFRTP was observed on the fractured surface of the CFRTP, and it enlarged with increasing tool rotation speed due to increasing the melting interval of PA6. **Fig. 9** shows the SEI of the fractured surface in the tool-passed zone on the A5052 side of fractured joint at the tool rotation speed of 2000 rpm. The fractured surface could be classified into three categories as shown in regions (a)-(c) of Fig. 9, based on the surface features. Fig. 10 (a)-(c) show the typical fractured morphologies of (a)-(c) in Fig. 9. **Fig. 10** (d)-(f) show the results of high magnification analysis using EDS in (a)-(c), respectively. In region (a), the residual CFRTP was not observed. As-ground surface of A5052 was observed, thereby, this region was mainly fractured at the joint interface due to the weak joining force. The liner C concentrations were also detected along the ground scratches in Fig. 9 (d). This indicated the anchor effect between the molten PA6 and the scratches on A5052. In region (c), not only the C distributions in whole area with weal intensity, which corresponding to the fractured PA6, but also carbon fibers were detected. In other word, a part of bulk CFRTP with exposed carbon fibers was observed, which corresponded to CFRTP base material fracture. The fracture passed through the CFRTP bulk near the interface. In region (b), bulk CFRTP also observed, however, the surface was smooth compared to region (c). These smooth features corresponded to the void inner surface, and therefore it is likely that the fracture would pass across the voids. **Fig. 11** shows area fractions of interface, CFRTP base material and void fractures, which were evaluated by the SEIs of the fracture surface on A5052 of fracture joints joined at tool rotation speeds of 1000, 2000 and 2500 rpm. The area fraction of the interface fracture decreased with increasing the tool rotation speed. At lower rotation speed, the temperature at the interface was too low and the melting time duration was too short to obtain enough wetting of molten CFRTP on the A5052. Therefore, CFRTP base material fracture ratio increased, and the interface fracture ratio decreased with increasing tool rotation speed from 1000 to 2000 rpm due to the decrease of the unjoined area. As the result, the tensile shear fracture load of the FLJ joint also increased with increasing the tool rotation speed in this range. The area fraction of the void fracture increased with increasing tool rotation speed. These voids would be generated by the thermal decomposition of PA6 by increasing the temperature at the interface and the melting interval at the higher tool rotation speed. As the results, the tensile shear fracture load of the FLJ joint decreased with increasing

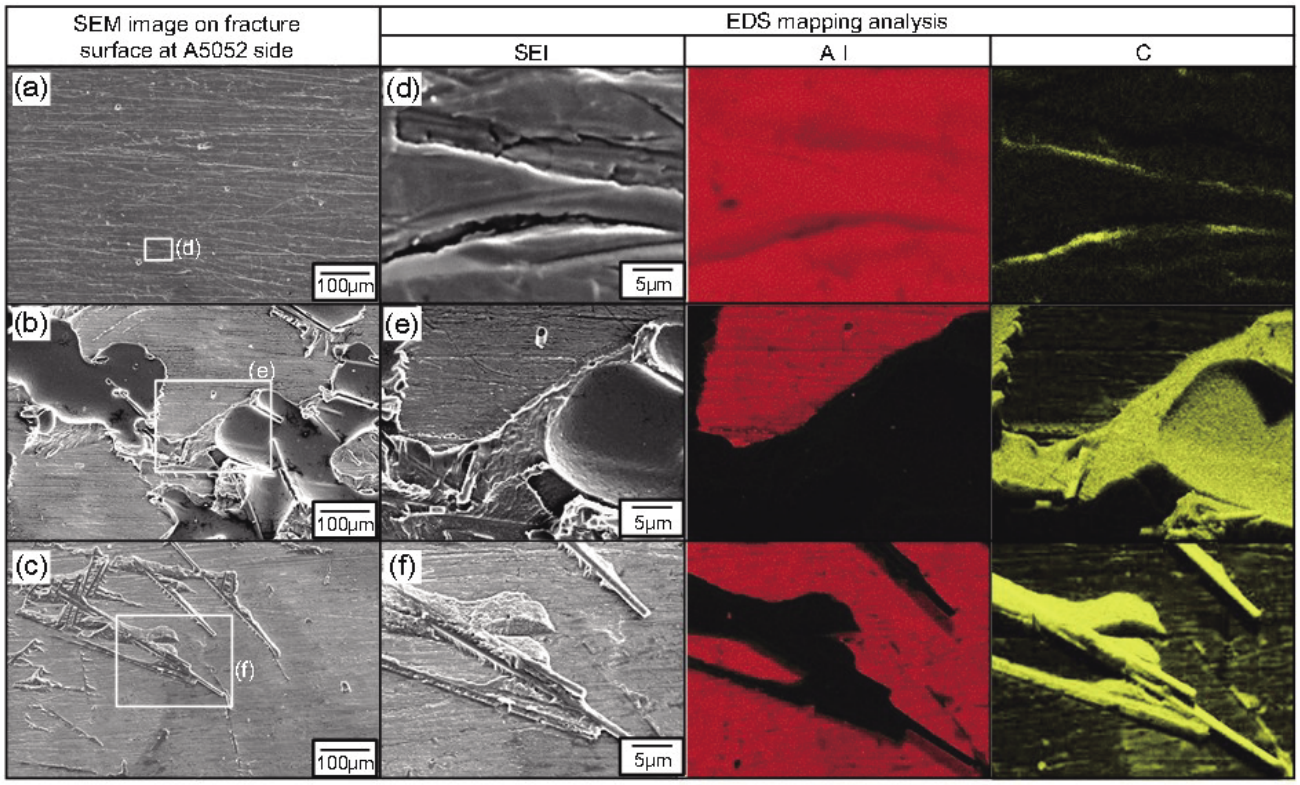

Fig. 10 (a)-(c) Typical fractured morphologies of regions of (a)-(c) in Fig. 9, and (d)-(f) results of high magnification analysis using EDS in Fig. 10 (a)-(c).

tool rotation speed from 2000 to 2500 rpm by the voids formation in CFRTP and the thermal decomposition of PA6 in CFRTP of the joint. Especially, the voids would induce a stress concentration in CFRTP during the tensile shear test, thereby, it would be act as an origination of the fracture.

4. Conclusions

Direct joining of a carbon fiber reinforced thermoplastic (CFRTP: PA6 + 20wt% carbon fiber) and A5052 Al alloy was performed using friction lap joining (FLJ). The effect of the tool rotation speed as the major process parameter on the joint characteristics was investigated. The following conclusive remarks were obtained.

(1) Continuous joined interface of A5052/CFRTP joint was obtained by FLJ. These materials were joined by bonding of MgO oxide layer of A5052 and PA6 as the matrix of CFRTP. Voids were observed in CFRTP at the interface of the joint, and its quantity increased with increasing tool rotation speed.

(2) The tensile shear fracture load of FLJ joint increased with increasing the tool rotation speed from 1000 to 2000 rpm, and then it decreased. The fracture mainly occurred at the joint interface, however, the residual CFRTPs which bonded to the fractured surface of A5052 side were observed. The area fraction of interface fracture

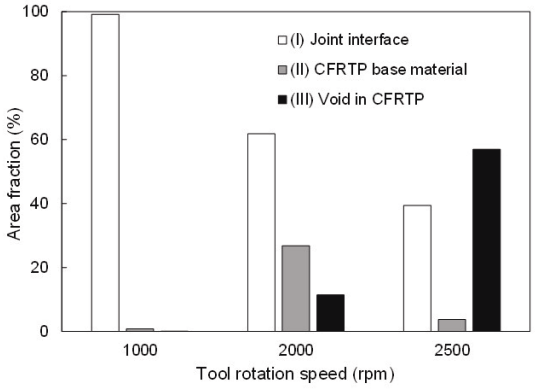

Fig. 11 Area fractions of interface, CFRTP base material and void fractures on the fractured surfaces of FLJ joints joined at tool rotation speeds of 1000, 2000 and 2500 rpm.

decreased with increasing the tool rotation speed. In addition, some joints joined at the tool rotation speed of 2000 and 2500 rpm showed the CFRTP base plate fracture.

Acknowledgements

This work was partly supported by Innovative Structural Materials Project (Future Pioneering Project) NEDO Project, Japan and JSPS KAKENHI Grant Number 26820326.

References

[1] J. C. Williams, and E. A. Starke Jr., Acta. Mater., **51** (2003) 5775-5799.
[2] H. Adam, Mater. Des., **18** (1997) 349-355.
[3] S. Y. Fu, B. Lauke, E. Mader, C. Y. Yue, and X. Hu, Compos. Part A, **31** (2000) 1117-1125.
[4] J. M. Arenas, C. Alía, J. J. Narbón, R. Ocaña, and C. González, Compos. Part B-Eng., **44** (2013) 417-423.
[5] J. P. Kabche, V. Caccese, K. A. Berube, and R. Bragg, Compos. Part B-Eng., **38** (2007) 66-78.
[6] A. Fink, P. P. Camanho, J. M. Andrés, E. Pfeiffer, and A. Obst, Compos. Sci. Technol., **70** (2010) 305-317.
[7] S. B. Kumar, I. Sridhar, S. Sivashanker, S. O. Osiyemi, and A. Bag, Mater. Sci. Eng. B, **132** (2006) 113-120.
[8] K. W. Jung, Y. Kawahito, M. Takahashi, and S. Katayama, J. Laser Appl., **25** (2013) 032003.
[9] M. Wahba, Y. Kawahito, and S. Katayama, J. Mater. Process. Technol., **211** (2011) 1166-1174.
[10] S. Katayama, Y. Kawahito, Scr. Mater., **59** (2008) 1247-1250.
[11] X. Tan, J. Zhang, J. Shan, S. Yang, and J. Ren, Compos. Part B-Eng., **70** (2015) 35-43.
[12] Y. Kawahito, S. Katayama, Trans. JWRI, **39** (2010) 50-52.
[13] K. W. Jung, Y. Kawahito, S. Katayama, Trans. JWRI, **42** (2013) 5-8.
[14] M. Hino, Y. Mitooka, K. Murakami, K. Urakami, H. Nagase, and T. Kanadani, Mater. Trans., **52** (2011) 1041-1047.
[15] F. Balle, G. Wagner, and D. Eifler, Mater. Werks., **38** (2007) 934-938.
[16] F. Balle, G. Wagner, and D. Eifler, Adv. Eng. Mater., **11** (2009) 35-39.
[17] F. Balle, and D. Eifler, Mater. Werks., **43** (2012) 286-292.
[18] P. Mitschang, R. Velthuis, S. Emrich, and M. Kopnarski, J. Thermoplastic Comp. Mater., **22** (2009) 767-801.
[19] S. T. Amancio-Filho, C. Bueno, J. F. dos Santos, N. Huber, and E. Hage Jr., Mater. Sci. Eng. A, **528** (2011) 3841-3848.
[20] F. Yusof, Y. Miyashita, N. Seo, Y. Mutoh, R. Moshwan, Sci. Tech. Weld. Join., **17** (2012) 544-549.
[21] F. C. Liu, J. Liao, and K. Nakata, Mater. Des., **54** (2014) 236-244.
[22] K. Nagatsuka, S. Yoshida, A. Tsuchiya, and K. Nakata, Compos. Part B-Eng., 73 (2015) 82-88.
[23] K. Nagatsuka, S. Yoshida, A. Tsuchiya, and K. Nakata, Conference papers of YPIC2014 (2014) 73-76.
[24] K. Nagatsuka, T. Onoda, T. Okada, and K. Nakata, Q. J. Jpn. Weld. Soc., 32 (2014) 235-241.
[25] F.C. Liu, J. Liao, Y. Gao, and K. Nakata, Sci. Tch. Weld. Join., 20 (2015) 291-296.
[26] Y. C. Chen, and K. Nakata, Scr. Mater., 25 (2008) 433-436.
[27] S. Straus, and L. A. Wall, J. Res. Nat. Bur. Stand., 63 (1959) 269-273.
[28] K. Ikeuchi, K. Kotani, and F. Matsuda, Q. J. Jpn. Weld. Soc., 14 (1996) 122-128.
[29] The adhesion society of Japan, Secchaku-handbook, fourth ed. Tokyo: NIKKAN KOGYO SHIMBUN Ltd. (2007) 834-863.
[30] W. P. Vellinga, G. Eising, F. M. de Wit, J. M. C. Mol, H. Terryn, J. H. W. de Wit, and J. T. M. D. Hosson, Mater. Sci. Eng. A, **527** (2010) 5637-5647.
[31] W. C. Wagner, and K. Asgar, J. Biomed. Mater. Res., **27** (1993) 531-537.